Anticancer activity of nanoencapsulated ginger in whey proteins against human tumor cell lines

Marwa M. Mounier[a], Samera Hassan Shehata[b], Tarek Nour Soliman[c]

[a]Pharmacognosy Department, Pharmaceutical and Drug Industries Research Division, National Research Centre (NRC), EL Buhouth St., Dokki, Cairo, Egypt, [b]Department of Dairy Science and Technology, Menoufia University, Shibin Elkom, Cairo, Egypt, [c]Dairy Department, Food Industries and Nutrition Research Division, National Research Centre El-Buhouth St., Dokki, Cairo, Egypt

Correspondence to Marwa M. Mounier, Pharmacognosy Department, Pharmaceutical and Drug Industries Research Division, National Research Centre (NRC), EL Buhouth St, Dokki, Cairo, Egypt. Tel: +201224646894; e-mail: marwa_m3@yahoo.com

Received: 28 June 2019
Revised: 11 July 2019
Accepted: 18 November 2019
Published: 30 June 2020

Egyptian Pharmaceutical Journal 2020, 19:87–96

Background and objective
Zingiber officinaleis, known as ginger, has been used in Arabic traditional medicine for its immense pharmacological effects. Encapsulation of the bioactive compounds is a powerful approach to improve their bioactivities, decrease their toxicities, and expand their physical steadiness. In this investigation, the cytotoxic activity of free and nanoencapsulated ginger against three human tumor cell lines was assessed with respect to IC50 and selectivity index. Additionally, the prompted apoptotic changes by free and nanoencapsulated ginger were evaluated.
Materials and methods
Ethanol extract was prepared from powdered ginger. Total phenol content was measured using the Folin–Ciocalteau method, where ginger extract (GE) (30 μl) was mixed with 2.37 ml deionized water, and then 150 μl Folin–Ciocalteau's phenol reagent and 450 μl sodium bicarbonate (20% w/v) were added to the mixture. Absorbance was measured at 760 nm. Preparations of GE-loaded in Whey protein isolate (WPI) were done through charged alkaline WPI solution by absolute ethanol.
Results
GE demonstrated the most powerful anticancer activity on breast cancer cells with high selectivity index (SI) and specificity. The particle size of WPI nanoparticles was 91.98 nm, which decreased by increasing the loading percentage of the ginger-extract reaching 73.47 nm with maximum loading. Conversely, the encapsulation efficiency (EE) of the encapsulated ginger-extract in WPI nanoparticles was 79.78%, which was increased by increasing the loading percentage of the ginger extract. Moreover, nanoparticle yield was higher than 78.45% for all samples. Encapsulation of GE enhanced the tumor suppression effect of the free GE. This may be attributed to the slow release and high solubility of the nanoencapsulated ginger.
Conclusion
Nanoencapsulation using WPI upgraded altogether the bioavailability of ginger and its anticancer action in comparison with free GE.

Keywords:
anticancer activity, bioavailability, cell line, ginger, nanoencapsulation

Egypt Pharmaceut J 19:87–96

1687-4315

Introduction

Zingiber officinale, known as ginger, has several health benefits. Ginger is commonly used as a spice, food, as well as medicinal agent in India, Asia, and Arabic traditional medicine [1]. The medicinal properties of ginger include anticancer, antioxidant, and anti-inflammatory activities [2], which has led to its wide use in numerous commercial natural products.

Milk constituents have been considered as practical components, where 'whey' has been perceived as a standout among the most wholesome and significant milk components. All whey protein gives states of essential and branched chain amino acids [3]. So, WPs have given some pharmacological effects useful to individuals. Whey proteins show very steady pharmacokinetic profile, as they can oppose the dangerous activity of stomach chemicals and survive the stomach acids without being denatured [4]. However, ingested whey proteins can reach the jejunum rapidly, so they are viewed as 'quick proteins.' After reaching the small intestine, they are hydrolyzed at a moderate rate, much slower than that of casein, which enables more noteworthy level of amino acids to be ingested over the entire length of the small digestive tract. In addition, whey protein has higher postprandial level for plasma amino acids than casein [4].

Desolvation is a straightforward, rapid, and easily applicable method for the preparation of

nanoparticles. This technique requires only two miscible solvents without the involvement of destructing factors such as high shear rate, heating, and sonication that can damage the tertiary structure of proteins. This procedure also does not include any toxic reagents and surfactants [5]. Nanoparticles when used in the biological and food systems may exhibit superior characteristics owing to microparticles, including unique quality, improved sensory properties, extended flavor perception, better mouth feel, transparent appearance, and enhanced process ability [6]. Therefore, nanobioparticles are prepared from generally recognized as safe biopolymers and are increasingly used for various applications in biomedical, pharmaceutical, and nutraceutical industries [3]. Hence, the purpose of this investigation was to consider the apoptotic anticancer effect of free and nanoencapsulated ginger in whey protein. These apoptotic changes are surveyed by estimation of tubulin polymerization, DNA fragmentation, Caspase 7, B-cell lymphoma 2 (BCL-2) family proteins (BCL-2, apoptosis regulator Bcl-2-associated X protein (BAX), and BAX/BCL-2 ratio), and tumor suppressor protein P53. The effect of nanoencapsulation on the bioavailability of ginger was likewise contemplated by in-vitro digestibility.

Materials and methods

Materials

Bipro whey protein isolate 92.6% protein (w/w) was obtained from Davisco Foods International Inc., Eden Prairie, USA. Sodium chloride (NaCl), sodium bicarbonate ($NaHCO_3$), sodium hydroxide (NaOH), hydrochloric acid (HCl), ethanol, and Folin and Ciocalteau's phenol reagents were purchased from Merck (Darmstadt, Germany). Bi-distilled water was used throughout the study.

Methods

Preparation of ginger extract

Ginger extract (GE) was prepared according to the procedure described previously [7]. Overall, 75 g of powdered ginger obtained from Harraz for food industry and natural products was percolated in 450 ml ethanol at ambient temperature. The extract was filtered using Whatman No.1 paper and then evaporated by high-vacuum until dryness and then stored at −20°C in glass vials.

Measurement of phenol content

Total phenol content was measured using the Folin–Ciocalteau method. GE (30 µl) was mixed with 2.37 ml deionized water and 150 µl Folin–Ciocalteau's phenol reagent and allowed to stand at room temperature for 7 min, and then 450 µl sodium bicarbonate solution (20% w/v) was added to the mixture. After standing for 70 min at room temperature, absorbance was measured (Spectrophotometer BioQuest CE2502; Cecil Instruments Ltd, Milton Technical Centre, Cambridge CB24 6AZ, England) at 760 nm. Results were expressed as mg gallic acid equivalents/100 g sample [8].

High-performance liquid chromatography analysis of polyphenols

High-performance liquid chromatography analysis was carried out using an Agilent 1260 series. The separation was carried out using Eclipse Plus C18 column (4.6 mm ×250 mm i.d., 5 µm). The mobile phase consisted of water (A) and 0.02% trifloroacetic acid in acetonitrile (B) at a flow rate 1 ml/min. The mobile phase was programmed consecutively in a linear gradient as follows: 0 min (80% A), 0–5 min (80% A), 5–8 min (40% A), 8–12 min (50% A), 12–14 min (80% A), and 14–16 min (80% A). The multiwavelength detector was monitored at 280 nm. The injection volume was 10 µl for each of the sample solutions. The column temperature was maintained at 35°C [9].

Preparation of extract-loaded particles

WPI was dissolved in 10 mmol/l-NaCl solution (3%, w/v) by stirring at 500 rpm at room temperature for 2 h, stored at 4°C for 12 h and then filtered through 0.45 µm polyvinylidene fluoride syringe filter (Whatman, Germany) before use. Protein solution was heated at 60°C for 30 min [10] and then GE was added at 0.06, 0.120, and 0.180 g to obtain 1 : 20, 1 : 40, and 1 : 60 core to shell of GE to WPI, respectively. The pH value was adjusted to 9.0 with 2 M NaOH, which led to smaller particles, based on preliminary experiments. The solution was then charged with ethanol at a rate of 1 ml/min while stirring at 500 rpm until the mixture became turbid. The rate of ethanol addition was controlled carefully as it influences the size of generated particles [11]. The amount of ethanol added was ∼3.3 ml per ml protein solution. Nanoparticles suspension was centrifuged at 16 700 rpm (refrigerated centrifuge model RS-20IV; Tomy Seiko Co. Ltd, Tokyo, Japan) for 10 min, and the obtained supernatant was used for the measurement of encapsulation efficiency. The resulting nanoparticles were then dried at −80°C and stored at −20°C until analyses.

Particles size measurement

Size and polydispersity of particles and capsules were determined by using a dynamic light scattering particle size analyzer (Zeta PAL; Brookhaven Instruments Co., Holtsville, New York, USA). For this purpose, dried samples were either dispersed in 10 ml ethanol at pH 9.0 or bi-distilled water with pH 9.0 at ratio of 1 : 200 (w/v) and shaken continuously at room temperature for 12 h using shaking incubator (Stuart, S150; Guill Bern Corporation Inc., Philippines) to allow complete hydration. To investigate the influence of heat treatment of WPI on particle size, a sample was also prepared from nonheated WPI following the same procedure as described. Particle size measurements were carried out at 25°C with laser beam operated at 657 nm and scattering angle of 90°. Each sample was read three times. Average sizes reported are the volume averaged diameters.

Particle yield and encapsulation efficiency

The weight of dried pellet of extract-free and extract-loaded particles was used for calculating the particle yield as follows:

$$\text{Particle yield}\% = \frac{\text{Weight of dry pellet}}{\text{Total weight of extract and WPI used for particles preparation}} \times 100$$

The encapsulation efficiency of extract was calculated as the difference between the total phenol content added to WPI solution before desolvation stage and the phenolic content remained in the supernatant.

In-vitro gastrointestinal digestion

Gastric digestion

The in-vitro gastric model protocol was adapted according to Guo *et al.* [12], with some modifications. Simulated gastric fluid (SGF) containing 2 g NaCl and 7 ml concentrated HCl was diluted to 1 l, and pH was adjusted to 1.2 using 1.0 mol/l HCl. Afterward, 14.93 mg pepsin was added to 7 ml SGF and held at 37°C with continuous shaking at 95 rpm in a temperature-controlled water bath (Grant OLS 200; Grant Instrument, UK) to mimic the conditions in the stomach. The pH and temperature were continuously monitored and controlled.

Freeze-dried ginger-loaded WPI (0.1 g) and WPI nanoparticles (Freeze dryer; Labconco, USA) were re-dispersed in 14 ml of SGF. Then, 7 ml of SGF containing pepsin was added to the mixture to make up a final volume of 21 ml (protein : enzyme ratio 1.87 : 1 w/w). The mixture was incubated at 37°C for up to 2 h, and samples were withdrawn at different time intervals for analyzing total phenol content at 760 nm, using ultraviolet-visible spectrophotometry to determine the released ginger. The pH of the mixture was maintained at 1.5 using 1 mol/l HCl. The digestion reaction was terminated by raising the pH to 7.0 with 0.1 mol/l NaOH before any analysis.

Gastrointestinal digestion

The in-vitro gastric model protocol was adapted according to Guo *et al.* [12], with some modifications. Aliquot (15 ml) of the sample solution containing nanoparticles with or without GE was mixed with 12.5 ml $NaHCO_3$ in which 56 mg pancreatin (P3292,4UPS; Sigma) and 0.35 g bile (B 8631; Sigma-Aldrich, Germany) were dissolved, and the pH of the sample was adjusted to 7 using NaOH (6 mol/l). Samples were incubated for 3 h, filtered through 0.45 μm filtration unit and analyzed for total phenolic content as described before to determine the released ginger.

Transmission electron microscopy

Samples were prepared for transmission electron microscopy (TEM) by fixation with glutaraldehyde as described by Moslehishad and Ezzatpanah [13], and then dilution (1 : 100 v/v) was carried out with deionized water. A drop of diluted suspension was placed on the sample holder called formvat-coated electron microscopy grid, left for 1 min, and then a drop of phosphotungstic acid solution (2% at pH: 7.2) was added. The grid was air dried and examined by TEM using a device called JEOL JEM-1400 plus TEM with an accelerating voltage of 100 kV at a magnification of ×200 000.

Cell lines

Human breast carcinoma (MCF-7 cell line), human colon carcinoma (HCT-116 cell line), human liver carcinoma (HepG 2), and skin normal human cell line (BJ-1) 'A telomerase immortalized normal foreskin fibroblast cell line' were obtained from Karolinska Center, Department of Oncology and Pathology, Karolinska Institute and Hospital, Stockholm, Sweden.

Cell culture

Culturing and subculturing were carried out according to Thabrew *et al.* [14]. Culture was maintained in RPMI 1640 medium with 1% antibiotic-antimycotic mixture (10 000 Ul/ml potassium penicillin, 10 000 μg/

ml streptomycin sulfate, and 25 μg/ml amphotericin B), 1% l-glutamine, and supplemented with 10% heat inactivated fetal bovine serum. Doxorubicin was used as a positive control. A negative control composed of dimethyl sulphoxide (DMSO) was also used.

Cell viability assay

The cells were seeded at concentration of 10×10^3 cells per well in case of MCF-7 and HepG2, 20×10^3 cells/well in a fresh complete growth medium in case of HCT-116, and 40×10^3 cells/well in a fresh complete growth medium in case of BJ-1cell lines using 96-well microtiter plastic plates at 37°C for 24 h under 5% CO_2, in a water jacketed carbon dioxide incubator [15]. Fresh medium (without serum) was added and cells were incubated either alone (negative control) or with samples to give a final concentration of 100 μg/ml. After 48 h of incubation, the medium was aspirated and then 40 μl MTT [3-(4, 5-dimethylthiazol-2-yl)-2, 5-diphenyltetrazolium bromide] salt (2.5 mg/ml) was added followed by the addition of 200 μl 10% SDS. The absorbance was measured at 595 nm.

Determination of IC_{50} and selectivity index values

IC_{50} values were calculated using the SPSS computer program (SPSS for windows, statistical analysis software package/version 9/1989; SPSS Inc., Chicago, Illinois, USA). The SI showed cytotoxic selectivity against cancer cells versus normal cells (BJ-1, skin human normal cell line).

Measurement of DNA fragmentation using diphenylamine) assay

DNA fragmentation of the cells was assayed, as described by Cohen and Duke [16], and Burton [17]. In brief, the cells were lysed with lysis buffer containing 20 mM EDTA, 0.5% (v/v) Triton X-100, and 5 mmol/l Tris-HCl (pH 8.0) for 15 min on ice. Intact chromatin (pellet) was separate from DNA fragments (supernatant) through centrifugation at 27.000 rpm for 15 min. The amount of DNA in both the pellet and the supernatant was measured at 600 nm using diphenylamine reagent. The percentage of DNA fragmentation was calculated as the ratio of DNA in supernatant and DNA in pellet.

Human CASP7 (Caspase 7) estimation

The precoated micro-ELISA plate with an antibody specific to CASP7 was used. Standards or samples were added to wells of this plate. Then, the biotinylated detection antibody specific for CASP7 and avidin–horseradish peroxidase (HRP) conjugate were added successively to each well and incubated. After washing, the substrate solution was then added. The enzyme–substrate reaction was terminated by the addition of sulfuric acid solution, whereas the color turned from blue to yellow. The optical density was measured at 450±2 nm [18].

Measurement of B-cell lymphoma 2 protein levels

The BCL-2 in samples and standards was allowed to bind to the antibody-coated wells of the plate. A biotin-conjugated antibody added to bind the protein was captured by the first antibody. Streptavidin-HRP was added to bind to the biotin-conjugated antibody. The substrate solution was added to the wells. The reaction was then terminated by addition of acid, and absorbance was measured at 450 nm. Protein concentration was measured from the prepared standard curve [19].

Measurement of Bax protein levels

Monoclonal antibodies were added to Bax immobilized on a microtiter plate to bind the Bax in the standards or samples. A recombinant human Bax-α standard was provided in the kit. After short incubation, the excess sample or standard was washed out, and a biotinylated monoclonal antibody to Bax was added. Streptavidin conjugated to HRP was added, which bounded to the biotinylated monoclonal Bax antibody. After short incubation, the enzyme reaction was stopped, and the color generated was read at 450 nm. The measured optical density is directly proportional to the concentration of Bax in either standards or samples [20].

Tubulin polymerization inhibition assay

Precoated plate with an antibody specific to Tubulin polymerization inhibition assay was used. Standards or samples were then added with a biotin-conjugated antibody specific to Tubulin polymerization inhibition assay. Then, addition of avidin conjugated to HRP was done. After TMB substrate solution was added, the enzyme substrate reaction was terminated by the addition of sulfuric acid solution, and the color change was measured spectrophotometrically at a wavelength of 450 ±10 nm [21].

Human P53 level estimation

An antihuman p53 coating antibody was adsorbed onto microwells. Human p53 present in the sample or standard binds to antibodies adsorbed to the microwells. A biotin-conjugated p53 antibody was added. Following incubation, streptavidin HRP was added and bounded to the biotin-conjugated

antihuman p53 antibody. Following incubation, the substrate solution reactive with HRP was added. A colored product was formed in proportion to the amount of human p53 present in the sample or standard. The reaction was terminated by addition of acid, and absorbance was measured at 450 nm [22].

Results and discussion

Particle size measurement

The polydispersity index of nano-WPI was 0.420, which decreased to 0.367 for encapsulated 60 mg GE, indicating more homogenous dispersity, as shown in Table 1. These results agree with the previous results for the encapsulation of the date palm pit extraction using WPI [23].

The mean particles size of the prepared WPI nanoparticles was 91.98±1.6 nm, which decreased by increasing the loading percentage of the GE reaching 73.47 nm at maximum loading (1 : 60) (Table 1). The results in Table 1 also indicated that the formation of nanoprotein particles via alcoholic desolvation was successful as all samples were in the nanoscale size. The results also showed that the particles size was progressively decreased with the increase in the loading percentage of GE. The negatively charged WPI particles exhibit repulsive forces among nanoparticles at alkaline pH to prevent particles aggregation. Heat treatment at 60°C of WPI developed significantly smaller particles, which may support the unfolding of WPI into a state referred to as molten globule [23]. Moreover, the increased pH before desolvation phase might keep the unfold WPI assemblies but exposing their hidden thiol groups to undergo thioldisulfide interchanges, without large particle formation [24]. All of these steps have aided in producing smaller particles and a more clear solution.

Table 1 Detection of polydispersity index, particle size, particle yield, and encapsulation efficiency of whey protein isolate nanoparticles and those at ratios of 1 : 20, 1 : 40 and 1 : 60 Whey protein isolate: ginger extract-loaded nanocapsules (20, 40, and 60, respectively)

Sample	PDI	Particle size (nm)	Particle yield (%)	Encapsulation efficiency (%)
WPI particles	0.420	91.98±1.6	78.45±1.06	–
20	0.344	85.94±1.3	90.09±0.17	79.78±2.78
40	0.387	78.08±1.7	93.41±1.81	82.37±3.25
60	0.367	73.47±1.5	95.04±0.13	72.45±1.75

PDI, polydispersity index; WPI, Whey protein isolate.

The nanoparticles yield was higher than that of the WPI (78.45%) for all samples (Table 1). This might imply the generation of suitable mass particles by the applied desolvation method [23,25]. There was a direct correlation between the particle yield and the percentage of added GE (Table 1).

The encapsulation efficiency of the encapsulated GE in WPI nanoparticles was 79.78% when the protein: GE ratio was 1 : 20, and increased to 82.37% when the ratio became 1 : 40 ratio, but decreased on further increase in the added GE (72.45%). This might be interpreted on the basis that protein–protein and polyphenol–protein interactions were reported to be weakened with increasing the extract-to-WPI ratio [25]. Similar conclusions were also reported for other biopolymer matrices, where the increases in the addition of the core material to the shell material were concomitant with a decrease in encapsulation efficiency [26].

Figure 1

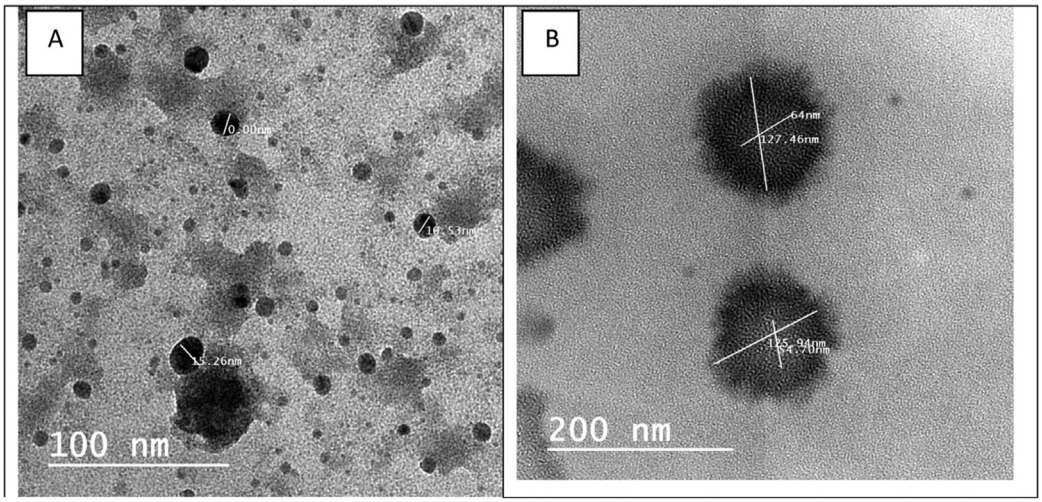

Transmission electron micrograph of (a) Whey protein isolate nanoparticles and (b) Whey protein isolate-ginger extract encapsulated.

Table 2 High-performance liquid chromatography analysis for polyphenols of ginger extract

Compounds	Area	Concentration (μg/g)
Coffeic acid	1.10	58.07
Syringic acid	2.71	142.61
Coumaric acid	3.59	188.96
Vanillin	3.93	206.78
Ferulic acid	2.32	122.34
Naringenin	0.46	24.16
Querectin	4.26	224.36
Cinnamic acid	0.77	40.55
Propyl gallate	1.54	81.08
4.7-Dihydroxyiso flavone	3.36	177.07

Transmission electron microscopy

The images of TEM showed that the nanoparticles of encapsulated GE retained a core/shell structure (Fig. 1), where the GE occupied the core with an average diameter of 127.46 nm, whereas WPI formed a 63 nm thick shell. This could be attributed to dehydration step of TEM leading to contraction of the examined particles.

High-performance liquid chromatography analysis of polyphenols

Further analysis for polyphenols of ginger extract is shown in Table 2. The assessments appeared that Quercetin represented the highest polyphenol constituent at 224.36 μg/l, followed by vanillin, Coumaric Acid, and 4.7-DihydroxyisoFlavone at 206.78, 188.96, and 177.07 μg/1, respectively. Moreover, the high-performance liquid chromatography test led to affirm the achievement of the extraction procedure and to know the substance of its principal components, which position the technique for encapsulation and its solid primary components.

In-vitro gastrointestinal digestion

Gastric digestion

During the intestinal digestion process, it is essential to control the release of the bioactive components from the delivery system. Encapsulating polyphenols in WPI as a delivery system preserves their biological activities from degradation. The percentage of polyphenols released in SGF from nanoparticles loaded with different concentrations of the GE is shown in Fig. 2a. The high and rapid release of ginger can be attributed to the relatively low molecular weights of ginger polyphenol components. However, the released nanoparticles retained the high percentage of the GE even after 120 min in the acidic medium. As expected, the percentage of the released GE increased with the increase of the loading ratio.

Gastrointestinal digestion

The obtained results indicated that nanocapsules containing 100 WPI and loaded 20 mg GE/g WPI had the lowest release of 95.78% which increased to 97.38% for 40 mg GE/g WPI, with the highest release of 99.24% for 60 mg GE/g WPI.

The released percentages of polyphenols from the WPI nanoparticles and simulated intestinal fluid ranged between 99.24 and 95.78% after 2 h, with a lower release percentage for the low loading addition of GE.

Ginger remained bonded to the WPI even after the changes in its microstructure have indicated the binding of the ginger to WPI was not dependent on the protein microstructure. This suggests that the interaction of ginger polyphenols and WPI was most probably through hydrogen bond in hydrophobic interaction as shown in Fig. 2b.

Cell viability assay

Cytotoxicity of free ginger extract

GE was recorded for its anticancer potentiality on human breast carcinoma (MCF-7 cell line), human colon carcinoma (HCT-116 cell line), and human liver carcinoma (HepG 2). The LC_{50} and selectivity according to SI values are shown in (Table 3). These outcomes demonstrated that GE had the most powerful anticancer activity on breast cancer cells with high SI and specificity. This apoptotic effect of ginger might be a direct result of the nearness of quercetin, vanillin, and coumaric acid. A few past investigations uncovered the anticancer properties of quercetin [27]. Vanillin was reported to induce apoptosis in human colorectal disease cells and to suppress metastasis of human malignancy cells [28]. Coumaric acid instigated decrease in cell reasonability and apoptotic effect in colon disease HT-29 and $CaCo_2$ [29].

Cytotoxicity of nanoencapsulated ginger

Three different concentrations (20, 40, and 60 mg) of nanoencapsulated GE were tested on breast cancer. Nanoparticles containing 20 mg GE (a) were more potent than capsules containing 40 mg GE (b) and 60 mg GE (c) with LC_{50} of 29.3, 60.3, and 66.4 μg/ml, respectively.

The apoptotic mechanism of free and nanoencapsulated ginger (a)

To figure out the molecular effect of ginger nanoparticles upon breast cancerous cells, few molecular parameters were measured to compare the effect of free and nanoencapsulated GE (20 mg).

Figure 2

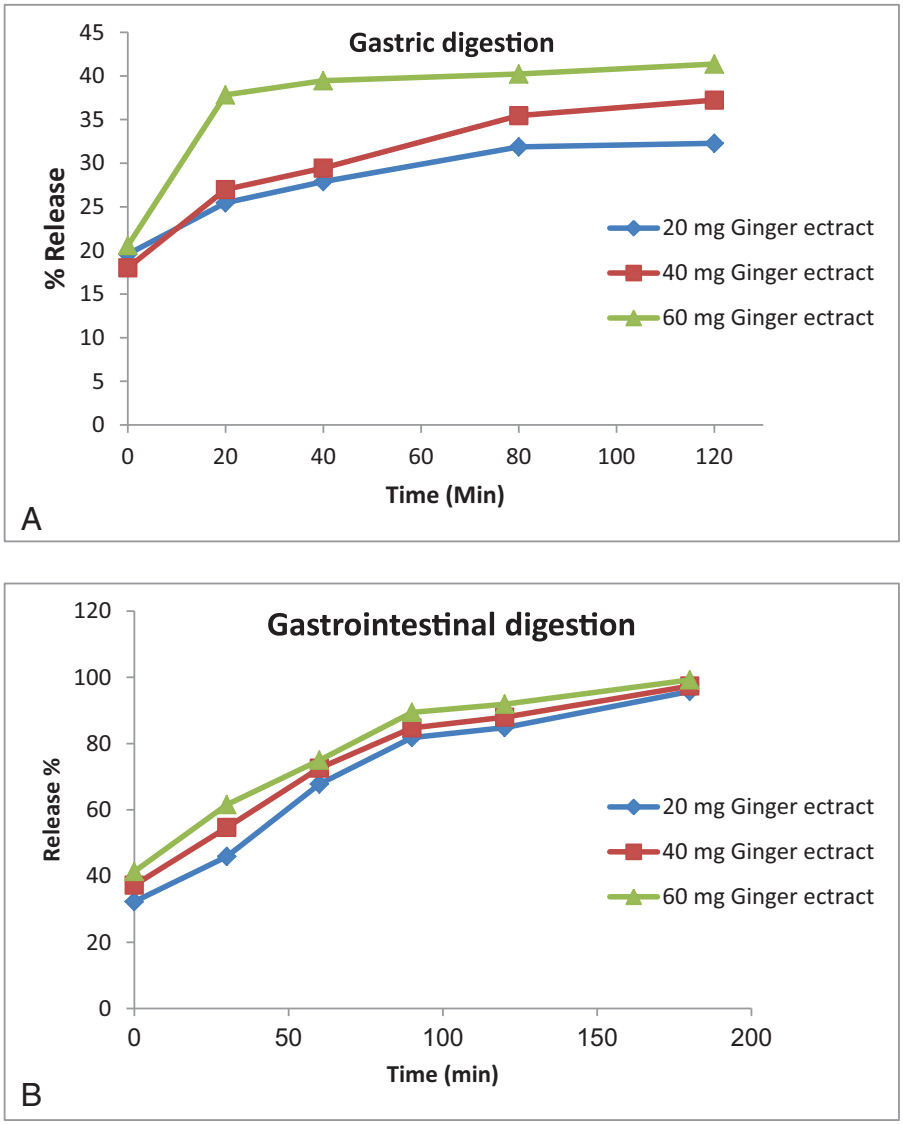

Release profile from ginger extract (a) in simulated gastric fluid and (b) in simulated intestinal fluid-loaded Whey protein isolate nanoparticles.

Table 3 Detection of LC_{50} and SI values of free ginger extract on breast (MCF-7), colon (HCT-116), and liver (HepG 2), values represented as±standard deviation (SD)

Sample	Cell lines	LC50	SI
Free Ginger Extract	MCF-7	14.5±0.9	2
Free Ginger Extract	HCT-116	18.3±1.3	1.6
Free Ginger Extract	HepG2	19.1±1.7	1.5

Table 4 Effect of MCF-7 cells treated with free ginger and ginger nanoencapsulated (A) on tubulin polymerization compared with controlled untreated MCF-7 and MCF-7 treated with reference drug colchicine

Samples	TubB IC50
Free ginger	6067.98
Ginger nanoencapsulated (A)	1026.644
Colchicine	487.7351

Encapsulated ginger inhibited the tubulin polymerization 5.9 folds than free ginger as shown in Table 4. The percentage of DNA fragmentation was increased inside cells treated with encapsulated ginger than the free ginger (Fig. 3). Encapsulated ginger upregulate protein level of caspase 7 and proapoptotic protein Bax (Figs 4–6) than the free GE. These results indicated that encapsulation enhanced the tumor suppression effect of the GE. This may be attributed to the slow release and high solubility of the nanoencapsulated ginger.

Conclusion

WPI nanoparticles and WPI-ginger-extract nanoencapsulated were successfully prepared at alkaline conditions. Heat treatment of whey proteins before the desolvation technique (charging by alcohol) process

Figure 3

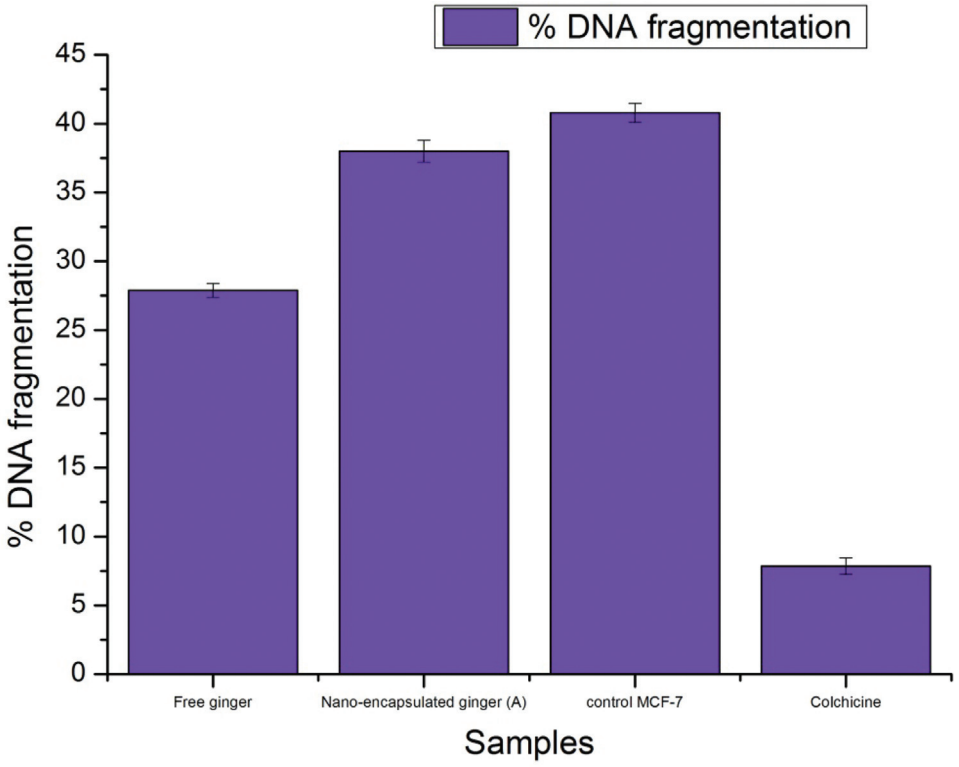

Percentage of DNA fragmentation in MCF-7 treated with free ginger and ginger nano-encapsulated (A) compared to untreated control MCF-7.

Figure 4

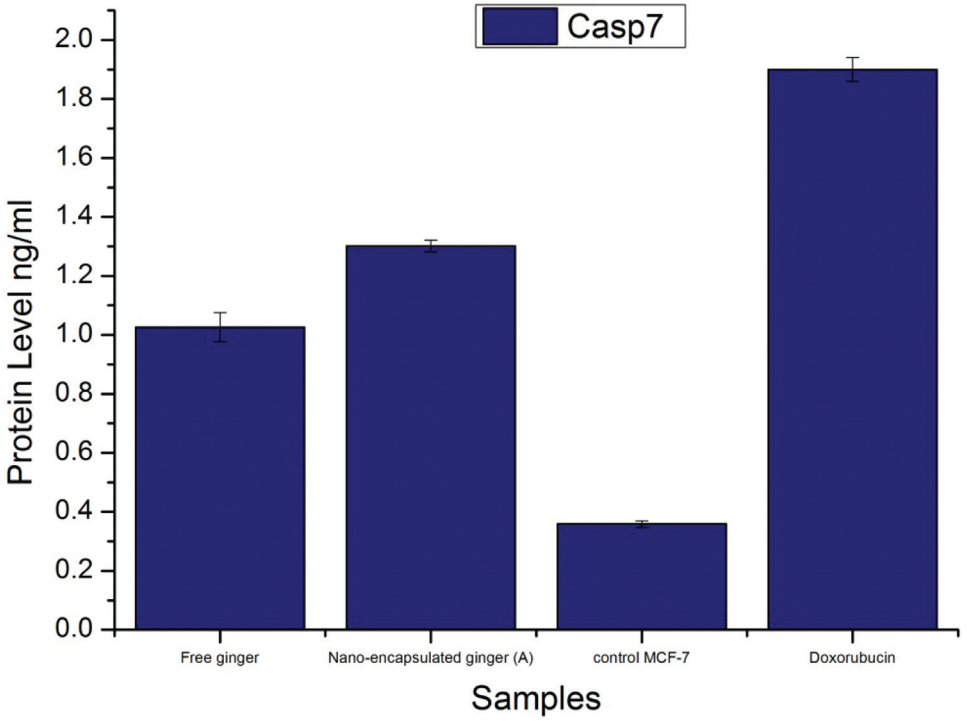

Effect of MCF-7 cells treated with free ginger and ginger nano-encapsulated (A) on Caspase7 compared to controled untreated MCF-7 and MCF-7 treated with reference drug doxorubicin.

decreased the mean size and increased the monodispersity and particle yield of extract-free and extracts loaded nanoparticles. An obvious efficiency for GE encapsulated by entrapment inside the WPI particles

Figure 5

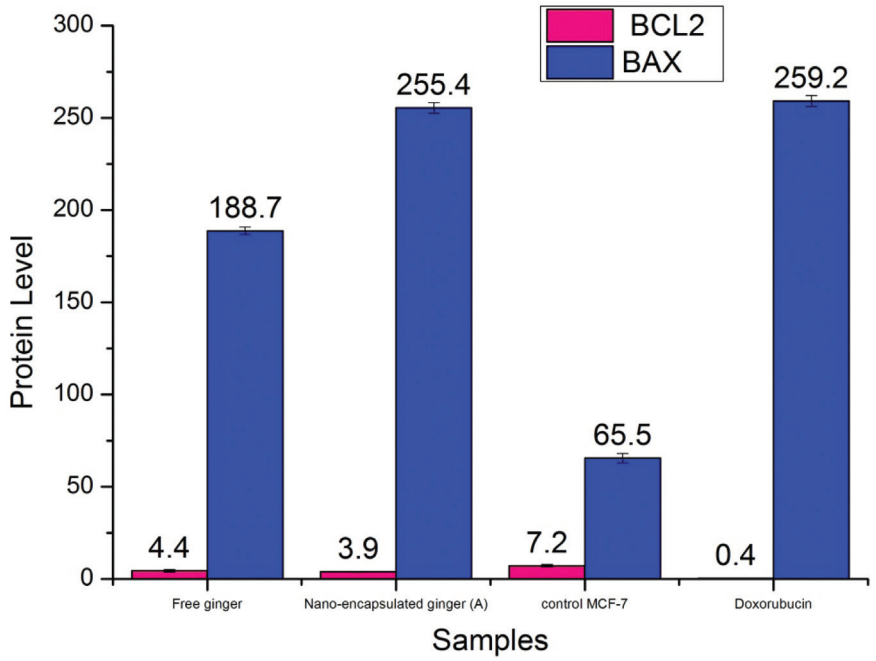

Effect of MCF-7 cells treated with free ginger and ginger nano-encapsulated (A) on BCL2 and BAX compared to controlled untreated MCF-7 and MCF-7 treated with reference drug doxorubicin.

Figure 6

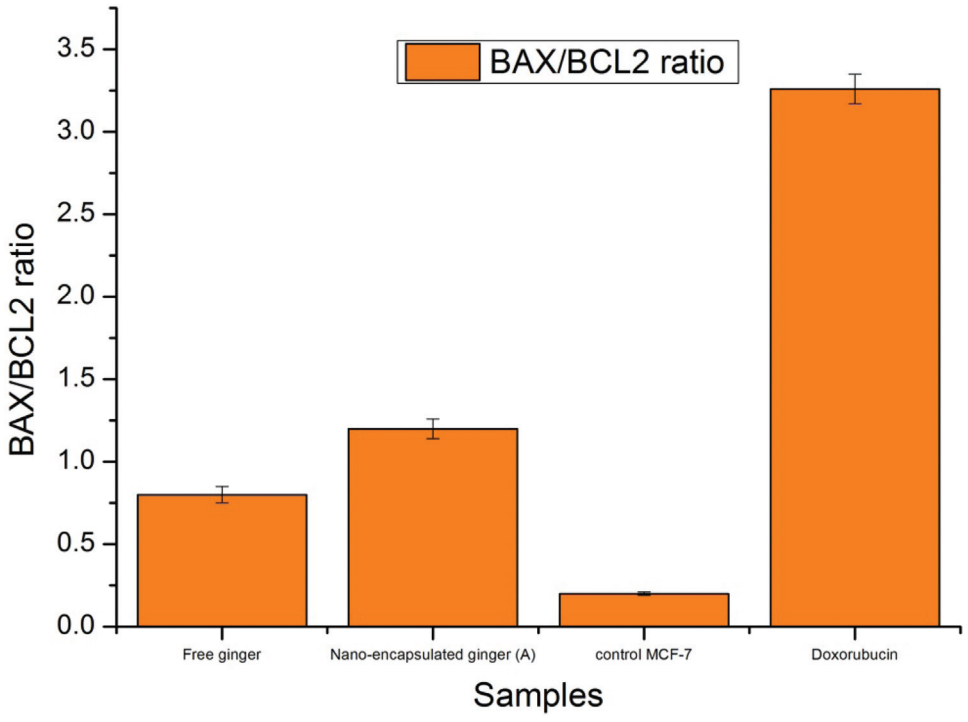

Effect of MCF-7 cells treated with free ginger and ginger nano-encapsulated (A) on BAX/BCL2 ratio compared to controlled untreated MCF-7 and MCF-7 treated with reference drug doxorubicin.

was achieved. Moreover, the study showed a higher mass ratio of core to the shell-forming protein produced lower particle yield and encapsulation efficiency. It was argued that because of over-loading, protein-protein and polyphenol–protein interactions were weakened at the higher GE-to-WPI ratio. WPI upgraded altogether the bioavailability of ginger by binding of the ginger to WPI. Nanocapsulation of ginger significantly enhanced its

anticancer activity through significant upregulation of proapoptotic BCL-2, increase % of DNA fragmentation, elevate caspase 7 level, disrupt BAX/BCL-2 ratio, enhance tubulin polymerization inhibition, and downregulation of BAX antiapoptotic protein in comparison with free GE.

Financial support and sponsorship
Nil.

Conflicts of interest
There are no conflicts of interest.

References

1 Račková L, Cupáková M, ⊠ažký A, Mičová J, Kolek E, Koš⊠álová D. Redox properties of ginger extracts: perspectives of use of *Zingiber officinale* Rosc.as antidiabetic agent. Interdiscip Toxicol 2013; 6:26–33.

2 Simon-Brown K, Solval KM, Chotiko A, Alfaro L, Reyes V, Liu C, *et al.* Microencapsulation of ginger (*Zingiber officinale*) extract by spray drying technology. LWT-Food Sci and Technol 2016; 70:119–125.

3 Almeida CC, Conte-Junior CA, Silva ACO, Alvares TS. Whey protein: Composition and functional properties. Encicl Bio 2013; 9:1840–1854.

4 Crinnion J. Whey Protein. Altern Med Rev 2008; 13:341–348.

5 Bilati U, Allémann E, Doelker E. Development of a nanoprecipitation method intended for the entrapment of hydrophilic drugs into nanoparticles. Euro J Pharmaceut Sci 2005; 24:67–75.

6 Moraru CI, Panchapakesan CP, Huang Q, Takhistov P, Liu S, Kokini JL. Nanotechnology: a new frontier in food science. Food Technol 2003; 57:24–29.

7 Moustafa SM, Mahmoud K, Menshawi BM, Wassel GM, Mounier MM. Cytotoxicity against four cell lines of human cancer by the fractionated extract of *Dovyalis caffra*, exhibiting high oxylipin signature, and by jasmine oil. World J Pharm Sci 2015; 3:580–587.

8 Shui G, Leong LP. Residue from star fruit as valuable source for functional food ingredients and antioxidant nutraceuticals. Food Chem 2006; 97:277–284.

9 Kim KH, Tsao R, Yang R, Cui SW. Phenolic acid profiles and antioxidant activities of wheat bran extracts and the effect of hydrolysis conditions. Food Chem 2006; 95:466–473.

10 Qi PX, Onwulata CI. Physical properties, molecular structures, and protein quality of texturized whey protein isolate: Effect of extrusion temperature. J Agri Food Chem 2011; 59:4668–4675.

11 Langer K, Balthasar S, Vogel V, Dinauer N, Briesen HV, Schubert D. Optimization of the preparation process for human serum albumin (HSA) nanoparticles. Inter J Pharm 2013; 257:169–180.

12 Guo Y, Harris P, Kaur A, Pastrana L, Jauregi P. Characterisation of ßlactoglobulin nanoparticles and their binding to caffeine. Food Chem 2017; 71:85–93.

13 Moslehishad M, Ezzatpanah H. Transmission electron microscopy study of casein micelle in raw milk with different somatic cell count levels. Int J Food Prop 2010; 13:546–552.

14 Thabrew M, Hughes RD, Mcfarlane IG. Screening of hepatoprotective plant components using a HepG2 cell cytotoxicity assay. J Pharm Pharmacol 1997; 49:1132–1135.

15 Raslan MA, Melek FR, Said AA, Elshamy AI, Umeyama A, Mounier MM. New cytotoxic dihydrochalcone and steroidal saponins from the aerial parts of Sansevieria cylindrica Bojer ex Hook. J Phytochem Lett 2017; 22:39–43.

16 Cohen JJ, Duke RC. Glucocorticoid activation of a calcium-dependent endonuclease in thymocyte nuclei leads to cell death. J Immun 1984; 132:38–42.

17 Burton K. A study of the conditions and mechanism of the diphenylamine reaction for the colorimetric estimation of deoxyribonucleic acid. Biochem J 1956; 62:315.

18 Denault JB, Salvesen GS. Human caspase-7 activity and regulation by its N-terminal peptide. J Biolog Chem 2003; 278:34042–34050.

19 Barbareschi M, Caffo O, Veronese S, Leek RD, Fina P, Fox S, *et al.* Bcl-2 and p53 expression in node-negative breast carcinoma: a study with long-term follow-up. Human Pathol 1996; 27:1149–1155.

20 Onur R, Semerciöz A, Orhan I, Yekeler H. The effects of melatonin and the antioxidant defense system on apoptosis regulator proteins (Bax and Bcl-2) in experimentally induced varicocele. Urolog Res 2004; 32:204–208.

21 Liliom K, Lehotzky A, Molnar A, Ovadi J. Characterization of tubulin-alkaloid interactions by enzyme-linked immunosorbent assay. Anal biochem 1995; 228:18–26.

22 Thomas MD, McIntosh GG, Anderson JJ, McKenna DM, Parr AH, Johnstone R, *et al.* A novel quantitative immunoassay system for p53 using antibodies selected for optimum designation of p53 status. J Clin Pathol 1997; 50:143–147.

23 Bagheri GH, Bonadonna C, Manzella I, Pontelandolfo P, Haas P. Dedicated vertical wind tunnel for the study of sedimentation of non-spherical particles. Rev Scien Instrum 2013; 84:054501.

24 Gunasekaran S, Ko S, Xiao L. Use of whey protein for encapsulation and controlled delivery applications. J Food Eng 2007; 83:31–40.

25 Zou T, Li Z, Percival SS, Bonard S, Gu L. Fabrication, characterization, and cytotoxicity evaluation of cranberry procyanidins-zein. Food Hydrocol 2012; 27:293–300.

26 Shah S, Pal A, Kaushik VK, Devi S. Preparation and characterization of venlafaxine hydrochloride-loaded chitosan nanoparticles and *in vitro* release of drug. J Appl Poly Sci 2009; 112:2876–2887.

27 Hashemzaei M, Delarami Far A, Yari A, Heravi RE, Tabrizian K, Taghdisi K, *et al.* Anticancer and apoptosis? inducing effects of quercetin *in vitro* and *in vivo*. Oncol report 2017; 38:819–828.

28 Naz H, Tarique M, Khan P, Luqman S, Ahamad S, Islam A, *et al.* Evidence of vanillin binding to CAMKIV explains the anti-cancer mechanism in human hepatic carcinoma and neuroblastoma cells. Molecul Cellul Biochem 2018; 438:35–45.

29 Rosa LS, Silva NJA, Soares NCP, Monteiro MC, Teodoro AJ. Anticancer properties of phenolic acids in colon cancer. A rev J Nutr Food Sci 2016; 6:10–4172.